ELSEVIER

Biophysical Chemistry 114 (2005) 43–52

Biophysical Chemistry

http://www.elsevier.com/locate/biophyschem

Ligand-linked stability of mutants of the C-domain of calmodulin

Kenosha F. Hobson, Nicole A. Housley, Susan Pedigo*

University of Mississippi, Dept. of Chemistry and Biochemistry, University, MS 38677, USA

Received 10 September 2004; received in revised form 5 November 2004; accepted 5 November 2004
Available online 21 November 2004

Abstract

There is a necessary energetic linkage between ligand binding and stability in biological molecules. The critical glutamate in Site 4 was mutated to create two mutants of the C-domain of calmodulin yielding E140D and E140Q. These proteins were stably folded in the absence of calcium, but had dramatically impaired binding of calcium. We determined the stability of the mutant proteins in the absence and presence of calcium using urea-induced unfolding monitored by circular dichroism (CD) spectroscopy. These calcium-dependent unfolding curves were fit to models that allowed for linkage of stability to binding of a single calcium ion to the native and unfolded states. Simultaneous analysis of the unfolding profiles for each mutant yielded estimates for calcium-binding constants that were consistent with results from direct titrations monitored by fluorescence. Binding to the unfolded state was not an important energetic contributor to the ligand-linked stability of these mutants.

Keywords: Ligand binding; Thermodynamic linkage; Calcium binding; Unfolded state; Partition function

1. Introduction

Ligand binding is an important factor in mediating biological activity of many macromolecules. Because of the propagated effects of ligand binding in macromolecules, there have been a number of studies that explore ligand linkage in other relevant equilibria such as stability, dimerization, and conformational change. This is the basis for several studies of the linkage of stability to proton binding [1,2], ion binding [3,4], and binding of cytidine-2′-monophosphate to Ribonuclease A [5]. It has been applied to the influence of ligands on conformational state [6–8] and dimerization [9]. The theoretical foundations have been laid for studying the relationship between ligand binding with different affinities to different states of a macromolecule, thereby influencing the position of equilibrium between these states [10,11]. Our laboratory is interested in the linkage between ligand binding and stability in calcium-binding proteins.

Calcium-binding proteins are well-suited to linkage studies. Calcium can be varied over a wide range of concentrations, and it does not interfere with typical spectroscopic signals from the protein. This paper reports linkage studies of mutants of the C-terminal domain of calmodulin in which Site 4 has been disabled by mutation of the terminal glutamate. These proteins provide excellent models with which to explore the linkage outlined in Scheme 1 and offer the following advantages.

(1) The proteins bind one ligand to the native state with moderate affinity that can be easily resolved from any low affinity events.
(2) The apo-proteins in the native state are folded to allow for measurement of the unfolding free energy in an independent experiment.
(3) The proteins have intrinsic spectroscopic signals for monitoring secondary structure and calcium binding.

The apo-native state (N) binds one calcium ion according to Reaction 1 to create the calcium-saturated native state (N·Ca). Both the apo-and calcium-saturated native states can be unfolded (Reactions 2 and 3) to form the apo-

* Corresponding author. Tel.: +1 662 915 5328; fax: +1 662 915 7300.
E-mail address: spedigo@olemiss.edu (S. Pedigo).

0301-4622/$ - see front matter © 2004 Elsevier B.V. All rights reserved.
doi:10.1016/j.bpc.2004.11.002

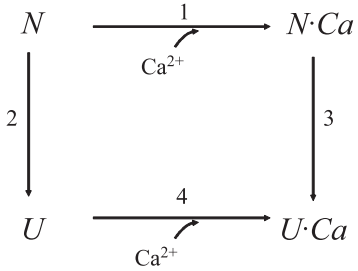

Scheme 1. Linkage of ligand binding to stability considering binding to unfolded state.

unfolded state (U) and the calcium-saturated unfolded state (U · Ca). Reaction 4 considers the possibility that a calcium ion binds to the unfolded state. The experiments described in this paper test this simple relationship between the native and unfolded states as a function of added ligand. A focus of this study is to determine whether it is necessary to consider ligand binding to the unfolded state (to form U · Ca) in order to adequately describe linked processes over a range of conditions. Although the C-domain of calmodulin offers a convenient spectroscopic signal for binding calcium to the native state, the studies presented here provide an option for inferring the ligand-binding constants in systems where a spectroscopic signal for the binding event is not available. This approach may be particularly useful in measuring weak interactions or those in which the spectral signals are not equivalent for each binding event.

Calmodulin is the quintessential member of the EF-hand family of calcium-binding proteins. Vertebrate calmodulin has four functional calcium-binding sites, two in each of two domains. The N-terminal domain contains Sites 1 and 2 and the C-terminal domain contains Sites 3 and 4. Although the domains are separated by a long central helix, they are known to influence each other both in the absence [12–14] and presence of physiological targets [15]. The domains can be separated by cleavage in the central helix region, but not without consequence to the calcium-binding properties of the sites in each domain [16–18]. Isolated N- and C-terminal domains are folded; they also bind calcium [16,17,19,20].

Foundations for this work were laid in a comprehensive study of the calcium-dependent stability of wild-type calmodulin and its isolated domains by Masino et al. [17]. The work reported here extends the studies of wild-type calmodulin in two important ways. Firstly, we bring to fruition the concepts introduced in that work to allow resolution of actual binding constants from unfolding data. This is important because it weaves theoretical and experimental approaches to allow characterization of each leg of the thermodynamic cycle depicted in Scheme 1. Secondly, we extend the work of Masino et al to include consideration of binding site mutants that bind only one ligand at mM levels of calcium, but have similar stabilities to wild-type. Consideration of only one ligand simplifies the analysis of the data allowing estimates of binding constants from unfolding data.

The proteins reported in this study are mutants of the isolated C-terminal domain of calmodulin (residues 76–148). The C-domain contains two EF-hand calcium-binding sites (Fig. 1A), Sites 3 and 4. In each of the mutants, Site 4 is impaired by mutation of the critical glutamate in position 12 (E140; Fig. 1B) to either glutamine or aspartate. Thus, we have created small, predominantly helical proteins that are soluble and bind nominally one calcium ion with moderate affinity to examine the thermodynamic linkage outlined in Scheme 1. This paper describes stability studies for E140D and E140Q, two mutants of the C-domain of calmodulin in the absence and presence of calcium. Calcium-binding constants for the native state, resolved from the unfolding studies, are compared to those determined independently in fluorescence experiments.

2. Experimental

2.1. Cloning

The expression plasmid for the C-domain of wild-type rat calmodulin (residues 76–148; denoted WT C-domain) was a kind gift of M. A. Shea (U. of Iowa). The gene was cloned into a pET7-7 vector between *Nde*I (5′end of gene) and *Bam*HI (3′end of gene) restriction enzyme sites [16]. Mutants were created using the Quickchange Mutagenesis Kit from Stratagene (LaJolla, CA). The instructions for the creation of mutagenic primers that were provided with the kit were followed to create two pairs of complimentary primers. Primers were synthesized, purified, and quantitated

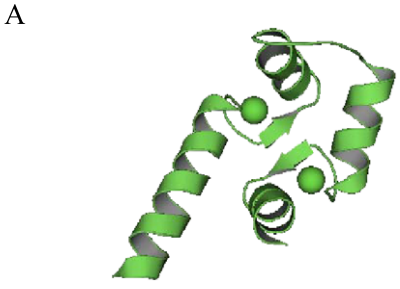

Fig. 1. Structure and sequence of C-domain of calmodulin. (A) Ribbon drawing of the Ca^{+2}-saturated C-terminal domain of calmodulin. The Cα-backbone of residues 76–148 from 3cln.pdb [31] are illustrated as a ribbon using PyMol (DeLano Scientific LLC; http://www.pymol.org). Calcium ions in each site are shown. Site 3 is to the left and Site 4 to the right. (B) Amino acid sequence of the C-domain of calmodulin from residues 76 to 148. The 12 residues of the calcium-binding site are highlighted (Site 3=residues 93–104; Site 4=residues 129–140) and aligned. The terminal glutamate (12th position), E140, is underlined and is mutated to either D or Q in the proteins studied here.

by MWGBiotech (Charlotte, NC). All controls specified in the mutagenesis kit were utilized. The DNA sequences of clones of wild-type and mutant proteins were confirmed at the University of Iowa DNA Facility. Expression plasmids were transformed into BL21(DE3) cells for overexpression. Cell stocks were frozen in 16% glycerol at −70 °C.

2.2. Overexpression and purification

Standard overexpression protocols were followed [21]. Briefly, a single colony from a streak of transformed cells on LB/agar-Amp (100 μg/mL) plates was used to inoculate an overnight culture (LB-Amp, 100 μg/mL). One-liter cultures (LB-Amp, 100 μg/mL) were supplemented with 50 mL of 1 M potassium phosphate, pH 7.4 and 20 mL of 20% glucose, then inoculated with 5 mL of the overnight culture. Large cultures were incubated at 37 °C for approximately 4 h before induction with 0.4 mM IPTG. Two hours post-induction, cells were pelleted by centrifugation and frozen until needed. Frozen cells were thawed and lysed by sonication. Calcium was added to the crude extract to 10 mM and the solution was heated to 80 °C for 10 min to precipitate impurities. Heat-treated material was cooled on ice for 10 min before centrifuging.

Soluble protein was purified by hydrophobic interaction chromatography on Phenyl Sepharose FF (Pharmacia) following a modified protocol of Putkey et al. [22]. Briefly, protein was adsorbed to the Phenyl Sepharose stationary phase in high-calcium/low-salt conditions followed by a step gradient to high-calcium/high-salt conditions. After returning to high-calcium/low-salt conditions, the protein was eluted in an EGTA/low-salt buffer. The protein was extensively dialyzed against water and lyophilized. The purity of the protein was greater than 95% as judged by Coomassie staining of SDS-PAGE gels.

2.3. Quantitation and characterization

A concentrated stock of each purified C-domain mutant was prepared by diluting 10 mg of lyophilized protein in 0.5 mL of water. This stock was diluted into a buffer comprised of 2 mM HEPES, pH 6.5, 100 mM KCl. The extinction coefficient for all mutant proteins at 280 nm was taken to be 2980/M/cm (data not shown). UV-vis spectra were consistent with a protein that contained no tryptophan. Circular dichroism (CD) spectra were taken (AVIV Stopped Flow Circular Dichroism Spectrometer-Model 202SF) in a 1-cm-path cell at 5 μM protein at 25 °C, 5-s averaging time, 1 nm band width from 300 to 200 nm with EGTA added to a final concentration of 20 μM in 2 mM HEPES, 0.1 M KCl, pH 6.5.

2.4. Stability studies

The decrease in helical signal upon addition of urea to the C-domain mutants of WT C-domain was monitored using CD at 222 nm. Constant volume titrations were performed by an automated titrimeter (Hamilton, Model Micrometer 500) in which the denaturant solution was titrated into the cuvette containing the native protein solution. The denatured and native protein solutions both contained equal concentrations of protein (~5 μM), HEPES (2 mM, pH 6.5), KCl (0.1 M), and either EGTA (20 μM) or calcium (0.1 mM to 10 mM) as specified in figure legends such that only the concentration of denaturant differed between the two solutions. The binding of calcium to the native state induces a realignment of the helices [23] that yields a greater CD signal at 222 nm [24,25]. The concentration of denaturant in the titrant solution was determined by refractive index according to the equations given by Pace [26]. All measurements were taken in a 1-cm quartz cuvette, stirred at 25 °C with 5-s averaging time.

There were factors that limited the range of calcium concentrations that could be explored in these experiments. The contaminating calcium concentration was determined by atomic absorption to be less than 10 μM. In order to create the apo condition, 20 μM EGTA was added to remove any calcium that was bound to the protein as well as the contaminating calcium. The lowest level of added calcium that could be reasonably explored was 100 μM. This was dictated by two factors: (1) the contaminating calcium was less than 10% of this value and (2) the concentration of the protein was 5 μM. Thus, if the protein were saturated, the free calcium concentration would change by 5% upon unfolding of the protein. The highest level of calcium that allowed resolution of both the folded and unfolded baselines was 1 mM. Unfolding data at 10 mM added calcium did not have an unfolded baseline.

The unfolding data were fit to a two-state model that assumed no thermodynamically relevant folding intermediates according to the equations below

$$K_{obs} = \frac{[U]}{[N]} = \frac{X_U}{X_N}; \quad X_U = \frac{K_{obs}}{1 + K_{obs}} \tag{1}$$

where K_{obs} is the equilibrium constant describing the ratio of concentrations of unfolded and native protein, and X_{U} is the mole fraction of the unfolded state and X_{N} is the mole fraction of the native state. The value of K_{obs} increases as denaturant is added according to the following linear equation [27,28]

$$\Delta G_{obs} = \Delta G^0_{un} - m_{\mathrm{D}}[\mathrm{D}] \tag{2}$$

where $\Delta G_{\mathrm{obs}} = -RT\ln K_{\mathrm{obs}}$ and $[D]$ is the concentration of urea. ΔG^0_{un} is the intrinsic stability of the protein in the absence of denaturant and the intercept of the linear plot of ΔG_{obs} vs. $[D]$. The m-value (m_{D}) is the sensitivity of the unfolding transition to the concentration of denaturant and the slope of the linear plot given by Eq. (2). Data were fit using IGOR Pro with procedure files written in-house as described elsewhere [29]. Data sets were fit individually

with all parameters allowed to vary (including the endpoints). All transitions appeared to be two-state as judged by the randomness of residuals of the fits (data not shown). Errors associated with resolved values are 68% confidence intervals.

2.5. Direct calcium titrations of mutant proteins

Tyrosine fluorescence was monitored on a Jobin Yvon Fluoromax 3 fluorimeter with the excitation at 277 nm and the emission at 308 nm with a 1-s averaging time at 25 °C. The titration was done by preparing 4 mL of protein solution at 2 μM total protein concentration in 20 mM HEPES, 100 mM KCl, pH 6.5. About 2 mL of the solution was placed in the cuvette and titrated with calcium by small volume additions of calcium chloride stock solutions. Contaminating calcium in our buffers was measured to be less than 10 μM using atomic absorption spectrometry (data not shown). The total calcium added was assumed to be equivalent to the free calcium. The low calcium endpoint was found by addition of EGTA to a final concentration of 1 mM to the remaining 2 mL of protein solution and measuring the fluorescence signal. Calcium titrations of WT C-domain were done using the technique of Tsien and Pozzan [30]. The presence of low levels of contaminating calcium precludes direct titration of WT C-domain because its binding affinity is higher than the mutant proteins.

Calcium binding was modeled as involving one calcium ion according to the chemical equation below:

$$\mathrm{N} + Ca^{2+} \leftrightarrow \mathrm{N}Ca \tag{3}$$

This equilibrium is governed by K_a, the calcium association constant which is related to the mole fraction of bound species (X_b) according to Eq. (4).

$$X_b = \frac{K_a[Ca^{2+}]}{1 + K_a[Ca^{2+}]} \tag{4}$$

Binding data were fit to Eq. (4) with adjustable slope and intercept endpoint parameters. The low calcium endpoints were not well defined in some of these titrations and were estimated based on the expected fluorescence signal enhancement upon the binding of calcium and the signal value at the high calcium endpoint (data not shown). The fluorescence signal of the sample before calcium was added was assigned a free calcium concentration of 10 μM based on results from atomic absorption. The sensitivity of results to this value was tested as follows. The value of contaminating calcium was varied over a 20-fold concentration range (1 to 20 μM). Binding free energies resolved from fits changed by 0.4 kJ/mol. Thus, because of weak calcium-binding affinity of the mutant proteins, results were not significantly affected by low levels of contaminating calcium.

2.6. Analysis of calcium-dependent urea-denaturation data

In order to resolve stability and binding free energies simultaneously, calcium-dependent urea-denaturation data were analyzed according to the following equations. The fraction unfolded is given by the equation below:

$$X_U = \frac{[U] + [UCa]}{[N] + [U] + [NCa] + [UCa]} \tag{5}$$

Binding of calcium to the unfolded state is modeled as a single ligand given by Eq. (6), which is governed by K'_a, the binding constant to the unfolded state.

$$\mathrm{U} + Ca^{2+} \leftrightarrow \mathrm{U}Ca \tag{6}$$

Thus, for our purposes here, we assume that there is only one "high" affinity calcium-binding site in the unfolded state. As we will discuss later, our data cannot support a more sophisticated model for binding to the unfolded state.

Eq. (5) can be reformulated in terms of the equilibria outlined in Eqs. (1), (4), and (6).

$$X_U = \frac{K_{obs} + K_{obs}K'_a[Ca^{2+}]}{1 + K_{obs} + K_a[Ca^{2+}] + K_{obs}K'_a[Ca^{2+}]} \tag{7}$$

The calcium-binding constants that are derived from Eq. (7) are the apparent calcium-binding constants that are determined from the shift in the urea-denaturation profile as calcium is added. In order to account for the effect of the denaturant upon the apparent calcium-binding constant, we used a linear equation in the same form as Eq. (4) as shown below:

$$\Delta G_a = \Delta G^0_a - m_a[D] \tag{8}$$

where ΔG_a is $-RT\ln K_a$, ΔG^0_a is the free energy for calcium binding in the absence of denaturant, and m_a is the slope of the dependence of the association free energy on denaturant.

Eq. (8) provides for a linear relationship between the binding free energy and the concentration of denaturant. This effect could be due to a change in accessible surface area or the effect of urea on the activity coefficients of interacting species including the effect of urea upon the activity of calcium. A linear free energy relationship is a first approximation and there may be higher order terms that we do not attempt to account for.

For the simultaneous analysis of the calcium-dependent urea-denaturation data, data sets were normalized to their endpoints from these individual fits. Normalized data for each protein were fit to Eq. (7) for which fixed endpoints, and ΔG^0_{un}, m_D, ΔG^0_a, m_a, and K'_a (allowed to vary) were global parameters. Selected results of fits to Eq. (7) are shown in Table 3. These results are also shown as the simulated curves in Fig. 4A and B. The data set at 10 mM calcium added is shown, but was not included in the simultaneous analysis (see below). The calcium concentration was a local parameter and that was fixed in each fit. In order to assess the effect of contaminating calcium on

resolved parameters, a series of fits was done in which the calcium concentration was fixed to the sum of the added calcium and the contaminating calcium (estimated to be 10 μM). Parameters resolved from these fits varied from those reported in Table 3 by 0.4 kJ/mol for the binding free energy (ΔG_a^0) and 0.06 kJ/mol/M in the m-value (m_a).

3. Results and discussion

3.1. Folded native apo-state

These experimental studies were designed to illustrate the thermodynamic linkage outlined in Scheme 1. Proteins that bind only one ligand allow for the most direct illustration of this linkage. Calmodulin is predominantly α-helical [31,32], which provides a convenient spectroscopic signal of the folded state. In addition, mutations of the critical glutamate in Site 4 of the C-domain were known to impair calcium binding, but not folding of the native state [33]. Thus, the proteins under study here (E140D and E140Q) were expected to be folded in the apo state. Mutations to the short β-sheet region of the C-domain were avoided since they are known to destabilize the apo state [34,35].

The CD spectra of the native apo-state (N) are shown in Fig. 2. The local minima at 208 and 222 nm indicate helical structure [36] indicating that these proteins are folded in the N state. The Q mutant yielded a lower signal (less negative) than the D mutant, but both are lower signals than observed for WT C-domain (data not shown). The relative positions of the CD spectra of E140D and E140Q are similar to those found for Site 3 variants in which acid pair variants were compared [37]. In those studies, variants with acidic groups in both the +Z and −Z positions [38] had a lower CD signal. Since the magnitude of the CD signal results not only from the helical content but also from the alignment of helices, it is difficult to assess the relative helical content of the mutants. However, these data are evidence that the N state of these proteins is folded to a significant extent.

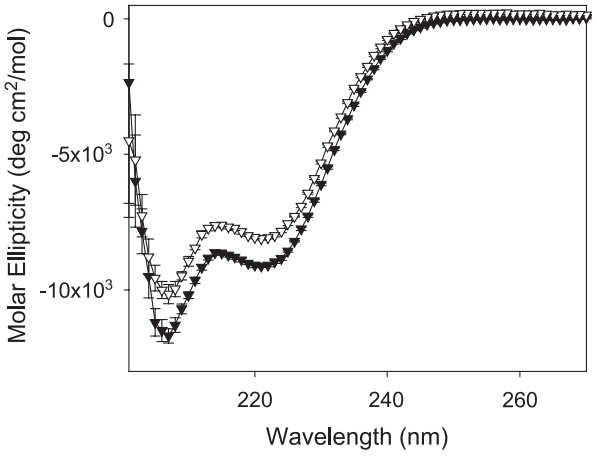

Fig. 2. Comparison of CD spectra of C-domain mutants. Data for each protein E140D (▼) and E140Q (▽) is shown with the error in the signal at each wavelength with a 5-s averaging time.

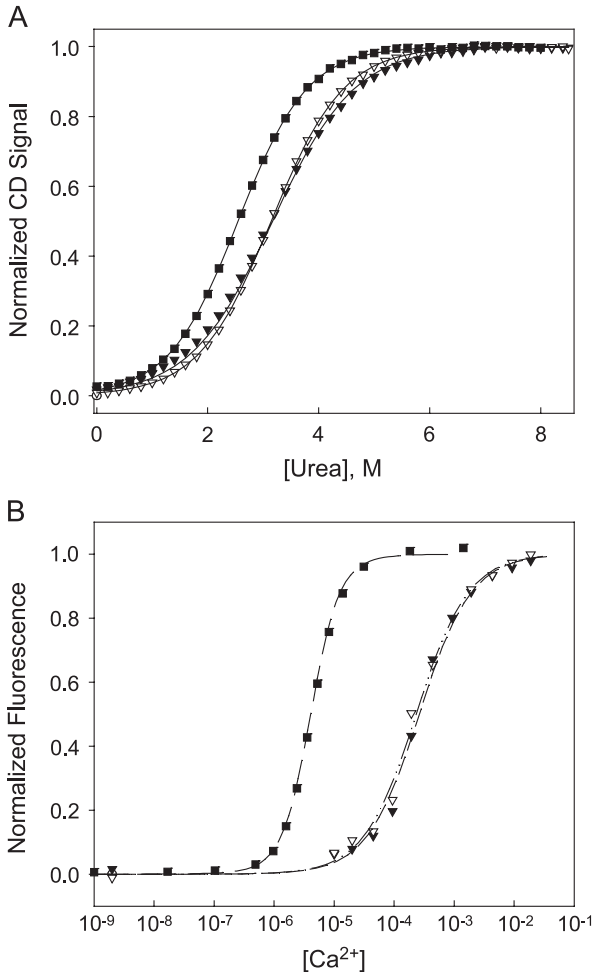

Fig. 3. Denaturation and calcium titrations of mutants of C-domain of calmodulin. (A) Urea denaturation of apo-state of each protein monitored by CD at 222 nm for E140D (▼), E140Q (▽), and WT C-domain (■). The solid lines are simulated transitions for each data set based on the best fit parameters to all replicates for each protein. (B) The normalized fluorescence signal is plotted versus the calcium added. The symbol types are the same as in Panel A. Each was fitted to the single site model (Eq. (4)). A simulated curve based on those fits is shown.

3.2. Stability of the native apo-state

Fig. 3A compares the urea-denaturation profiles for the wild-type and mutant proteins. It is clear from this profile that the Site 4 mutants are more stable than WT C-domain. The results from analysis of the proteins are presented in Table 1. The mutations stabilized the protein. We resolved free energies for E140D that were closer to that found for WT C-domain; however, ΔG_{un}^0(E140D) was greater than ΔG_{un}^0(WT C-domain) by 0.5±0.2 kJ/mol. The ΔG_{un}^0value for E140Q was 1.9±0.4 kJ/mol greater than that for WT C-domain. One explanation for the greater stability of the E140Q protein is that it has fewer negative charges in the

Table 1
Results from analysis of individual equilibria

	Urea denaturation[a]		Ca^{2+}-titration[b]
Protein	ΔG^0_{un}(kJ/mol)	m_G (kJ/mol/M)	ΔG^0_b (kJ/mol)
E140D	10.59±0.08	3.34±0.03	−20.4±0.3 (3800 M^{-1})
E140Q	11.97±0.04	3.83±0.01	−20.5±0.4 (3900 M^{-1})
WT	10.1±0.2	3.97±0.09	−30.7±0.08 (24,600 M^{-1})[c]

[a] Analysis of urea denaturation of protein with EGTA added according to Eqs. (1) and (2) at 25 °C.
[b] Binding free energy resolved from analysis of direct titrations of proteins monitored by fluorescence. Values in parentheses are the association constants based on the best-fit value for free energy change.
[c] Calcium binding to WT C-domain is cooperative with ΔG_1=−27.6±0.4 kJ/mol and ΔG_2=−61.50±0.08 kJ/mol. If we assume that the two sites are of equal intrinsic affinity, k is 35,000 M^{-1} and k_{34} (cooperativity between Sites 3 and 4) is 50.

binding site in the apo state. This is consistent with reports for oncomodulin mutants in which mutations that increased the number of negative charges in the EF-hand sites of oncomodulin caused a decrease in T_m [39].

Table 2 contains the nonpolar and polar accessible surface areas for unfolded and native WT C-domain in the apo and calcium-saturated states. These values for Accessible Polar and Nonpolar Surface Area for the folded states (Apo and Ca^{2+}-saturated) are greater than values for other proteins of equivalent size [40,41]. This indicates that the domain is not very compact. Expected m-values were calculated from these values according to Myers et al [40]. For the N to U transition, m_D is predicted to be 3.6 kJ/mol/M. This value compares well with the m-values for the WT C-domain and mutant proteins noted in Table 1.

3.3. Direct measurement of calcium binding using fluorescence

Calcium binding to the C-terminal domain of calmodulin was monitored through associated conformational change around Y138 [42]. Although this residue is located in Site 4, it reports on the binding of ligand to both Sites 3 and 4 [12]. Mutant proteins were titrated directly by making calcium additions to buffered protein solutions. Data were normalized and results of fits to Eq. (4) are presented in Fig. 3B along with simulated curves based on resolved parameters. Resolved free energy changes are reported in Table 1 and are the average of two to four independent determinations. The simplest interpretation of these results is that E140D and E140Q bind ligand with very similar average affinity of ~4000/M. The data for the WT C-domain is shown for comparison purposes. It binds two calciums cooperatively and with higher affinity. The fluorescence signals for the mutant proteins plateau in the mM range. There is no evidence for binding of a second ligand to the native state from these experiments.

From the direct titration experiments the affinity for calcium to Sites 3 (k_3) and 4 (k_4) can be estimated from the wild-type titration as noted in the footnote to Table 1 (k_3=k_4=k=35,000/M). These results (at pH 6.5) are similar to those from model-dependent analysis of fluorescence data of the identical construct by Sorensen et al that indicated the intrinsic affinity of Sites 3 and 4 (assuming that they are equal) is ~50,000/M at pH 7.5 [16]. Masino et al. [17] reported estimates of intrinsic affinity of 22,000/M at pH 8.0 and 22 °C (assuming a cooperativity of 50). Site 3 has been shown to be slightly higher affinity than Site 4, but only by a factor of 1.13 [43]. Thus, the assumption of equal intrinsic affinities for Sites 3 and 4 is a reasonable approximation, and our results for WT C-domain compare well to results from the literature under similar experimental conditions.

Mutation of the terminal glutamate in a site disables binding to that site such that it remains unbound unless extreme calcium concentrations are explored (>mM). Studies by Babu et al. [44] on D and Q mutations of the terminal glutamate in Troponin C showed that there were only three ligands bound at calcium concentrations up to 0.3 mM. Maune et al. [12] reached the same conclusion for Q mutants for Drosophila calmodulin according to flow dialysis studies, whereas UV difference studies showed that the signal of the tyrosine continued to change over four calcium ions per protein (1 mM final calcium concentration). In wild-type yeast (*Saccharomyces cerevisiae*) calmodulin, although a fourth ligand did not bind at calcium concentrations up to 0.3 mM [45], calcium continued to change the ϵ-proton signals of H107 up to 34 mM calcium added [46]. Thus, we believe that our mutant proteins bind only one calcium in the range of nM to mM.

The calcium-binding affinities resolved for the mutant proteins can be interpreted in terms of the intrinsic affinity of the unmutated site. That is, if the intrinsic affinity in Site 3 is unaffected by a mutation in Site 4, the E140Q and E140D mutants would have the same binding affinity for calcium and that binding affinity would be equal to the intrinsic affinity of Site 3 for calcium (~4000/M). Assuming Sites 3 and 4 have equal intrinsic affinity, we would expect the binding affinity to be ~35,000/M based on the WT C-

Table 2
Accessible nonpolar surface area for each of the three known states of the WT C-domain

State	Accessible nonpolar surface area (Å^2)	Accessible polar surface area (Å^2)
Unfolded	6580[a]	5843[b]
N[c]	2221	2726
$N \cdot Ca$[d]	2673	2617

[a] Calculated based on amino acid composition and the nonpolar surface area values of Chothia [55] and Livingstone et al. [56]. Value for the D mutants is 6568 Å^2. Value for Q mutants is 6577 Å^2.
[b] Calculated by subtraction of Accessible Nonpolar Surface Area from the total Accessible Surface Area according to Miller et al. [41].
[c] Calculated by *sracer* [57] based on a truncated version of 1cmf.pdb [58] containing only residues 76 to 148 with a probe radius of 1.5 Å.
[d] This nomenclature refers to the calcium-saturated state (2 Ca^{2+}/protein for WT C-domain). Calculated by *sracer* [57] based on a truncated version of 3cln.pdb [31] containing only residues 76 to 148 with a probe radius of 1.5 Å.

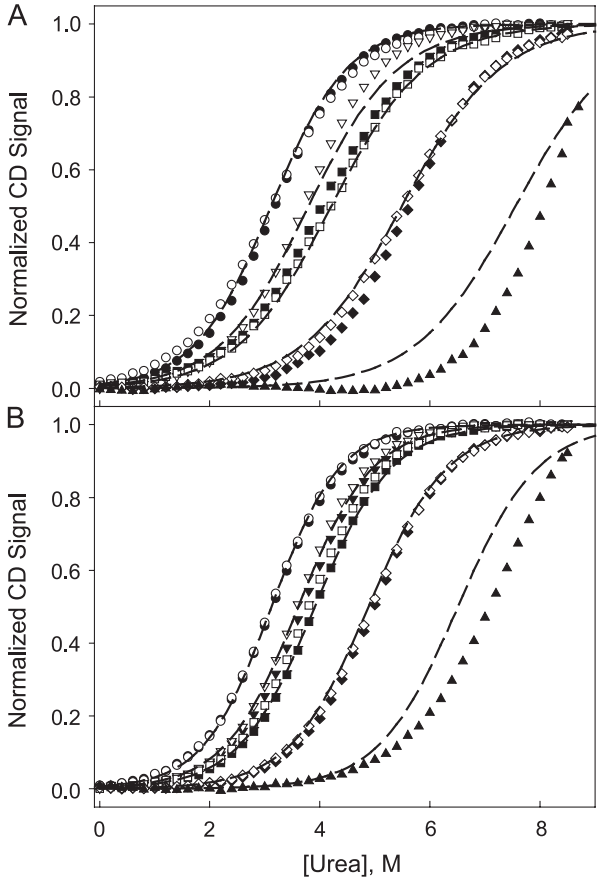

Fig. 4. Urea-denaturation of E140D (A) and E140Q (B). The normalized CD signal is shown for the following calcium concentrations: 20 μM EGTA (Apo-state; ●), 0.100 (▽ ▼), 0.200 (□■), 1 (◇◆), and 10 mM Ca^{2+} (△ ▲). Simulated curves are shown that are based on parameters resolved from fits to 1-Site Model (Eq. (7)) with K'_a fixed to 0 (dotted) as reported in Table 3.

domain data (footnote to Table 1). This value is similar to binding affinities for E140Q mutants of whole *Drosophila* calmodulin [12]. Thus, our results show an order of magnitude lower affinity binding to Site 3 than one might expect, indicating that the mutation at E140 has global effects upon the binding properties of the domain.

The molecular context of the C-terminal domain and the functionality of the sites in the domain both impact the calcium-binding affinity for the sites. There have been several studies of calmodulin variants, both engineered and natural, that address this issue. Starovasnik et al showed that mutation of the critical glutamate in one EF-hand site of Drosophila calmodulin had a deleterious affect on the other site in that domain [46]. In addition, the calcium affinity of Site 3 in yeast calmodulin (*S. cerevisiae*) is sensitive to the context of the domain. In whole yeast calmodulin, the C-terminal domain residues display slow exchange behavior on the NMR time scale. These same resonances displayed fast exchange behavior in the C-terminal tryptic fragment indicating that the calcium-binding affinity of Site 3 decreased in the isolated domain [47]. In addition, a factor of 4 difference in the calcium-binding affinity has been observed in the N-terminal domain of rat calmodulin due to a five-amino acid addition to the C-terminus of the N-terminal domain fragment [18,48]. Finally, the D133E mutation in Site 4 of whole calmodulin (+Z position in Site 4) decreased the calcium-binding affinity of Site 3 by a factor of 24 and of Site 4 by a factor of 2700 [37]. Thus, the observed calcium-binding affinity of the E140 mutant proteins is dependent upon the mutation and the context of the domain.

3.4. Calcium-dependent urea-denaturation of mutant proteins

Fig. 4A and B present the urea-denaturation data as a function of calcium concentration for both Site 4 mutants. For each set of unfolding curves, one can see that calcium stabilizes the proteins such that more denaturant is required to unfold the proteins at higher calcium concentrations. Unfolding profiles span a range of 6 orders of magnitude of calcium concentration (from nM to mM added calcium).

The values for ΔG^0_{un} and m_D from the simultaneous analysis of the calcium-dependent urea-denaturation data (Table 3) are only slightly higher than those values resolved from analysis of the apo-state data alone (Table 1). When K'_a (binding to the unfolded state) was allowed to vary, it returned a small negative number (~−200 for E140D and E140Q; data not shown). Since a negative binding constant is physically unreasonable, the parameters reported in Table 3 resulted from fits in which K'_a was fixed to 0. This is equivalent to removing the [U·Ca] term from Eq. (7). For the N·Ca to U transition, the *m*-value is predicted to be ~3.50 kJ/mol/M [40] using values for accessible surface area for WT C-domain. Thus, as the proteins are saturated with calcium, the hydrophobic cleft region is exposed and the unfolding transition represents a smaller change in exposure of hydrophobic surface area. This leads to a smaller predicted *m*-value than seen upon denaturing of *N*.

There is excellent agreement between the binding free energies resolved from simultaneous analysis of the calcium-

Table 3
Parameters resolved from simultaneous analysis of calcium-dependent urea denaturation experiments[a]

Protein	ΔG^0_{un}(kJ/mol)[b]	m_D (kJ/mol/M)[b]	ΔG^0_a (kJ/mol)[c]	m_a (kJ/mol/M)[c]
E140D	11.09±0.04	3.56±0.04	−20.9±0.3 (4600 M^{-1})	0.83±0.08
E140Q	12.51±0.03	4.01±0.04	−21.8±0.3 (5200 M^{-1})	0.59±0.04

[a] Analysis of calcium-dependent urea denaturation data (Eq. (7)). Binding constant to the unfolded state K'_a was fixed to 0.
[b] Stability and slope parameters (Eq. (2)).
[c] Binding free energy and slope parameters (Eq. (8)).

dependent urea-denaturation data and the direct titration data for both mutants. The agreement between these values was significantly poorer if the urea dependence of the binding constant (Eq. (8)) was not taken into account in the simultaneous analysis of the calcium-dependent urea-denaturation data.

We can predict the value of the linear dependence of the calcium-binding free energy on denaturant based on the change in the accessible surface area upon binding of calcium to the wild-type protein. We would expect that the value for m_a would be small and positive in that the total surface area increases as the protein binds calcium (ΔASA=344 Å^2). For the U to N·Ca transition, the change in Accessible Polar and Nonpolar Surface Area (Table 1) can be used to predict m_a arriving at a value of 0.25 kJ/mol/M [40] for WT C-domain. This would predict that the apparent binding free energy change should become more negative in the presence of urea. Values for m_a resolved from the fits to the data as reported in Table 3 are small and positive. Thus, there was agreement in the predicted *m*-value and experimental m-value for the mutant proteins.

The data set at 10 mM calcium added is shown in Fig. 4 for each of the mutant proteins. These data were not included in the simultaneous analysis. In fits where they were included, resolved parameters changed slightly, but the values of χ^2 increased 10-fold and there was still profound lack of fit for the 10 mM data set in spite of an increased m_a value. Simulations (data not shown) indicate that the displacement of the 10-mM data set to higher denaturant concentrations can be explained by binding of another ligand to the native state at high calcium concentration. This is the same concentration regime in which we might expect binding to the unfolded state to be manifested. The constants for binding of the second ligand to the native state and a ligand to the unfolded state are correlated in the analyses and cannot be independently resolved.

3.5. Binding to the unfolded state

Calcium has a preferred geometry for the chelating groups around the metal center; that is, either six ligands in trigonal bipyramidal geometry or seven ligands in pentagonal bipyrimidal geometry [49]. The coordinating waters are lost during the binding of calcium into a native state site [23,31]. It is unlikely for calcium to bind to the unfolded protein, release its waters as they are replaced by groups in the protein, and not induce a conformational change in the protein. The geometrical requirements for the chelating groups of calcium are too specific for this to happen without gross conformational change in the protein. However, one can imagine the possibility of several weakly associated calcium ions due to the predominance of acidic residues in the protein [50].

There are a number of references from the literature that note conformational change or heats of binding of divalent cations to calmodulin above the four calciums that binding to the EF-hand sites. Gilli et al. [51] performed flow dialysis

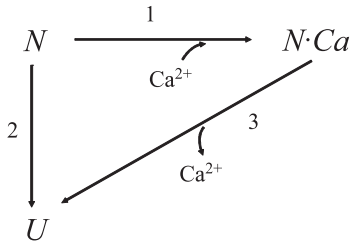

Scheme 2. Revised linkage of ligand binding to stability considering relevant equilibria.

experiments in which calcium ions continued to bind to SynCaM as the calcium concentration was increased with up to an 8 Ca^{2+} to 1 calmodulin ratio at 1 mM calcium. These results were confirmed in mass spectroscopic studies in which they found 4 to 6 auxiliary sites for binding of calcium [52,53]. Milos et al. [53] estimated the binding constants for Zn^{2+} in the presence of calcium to be approximately mM. Calmodulins engineered with a tryptophan reporter group in each binding site showed spectral changes at stoichiometries greater than four calciums per calmodulin [43]. High-resolution structural studies of Paramecium calmodulin showed a 5th calcium ion associated with the saturated structure that was important in the crystal lattice contacts [54]. Although these studies do not illustrate binding of cations to calmodulin in the unfolded state, they do show that there is cation association with calmodulin in regions outside of the EF-hand sites.

Binding to the unfolded state is not a significant contributor to the energetics of the linkage presented in Scheme 1. Thus, the linkage under study here would be better represented by Scheme 2 in which the U·C*a* state is not significantly populated.

In summary, these studies show that one can extract free energies of unfolding and calcium-binding constants from simultaneous analysis of urea-denaturation data if the binding free energy is corrected for the effect of urea. This is critical for systems in which binding is not easily measured through direct titrations due to a lack of convenient spectroscopic signals. The relatively simple calcium-binding proteins studied here provided a useful illustration of the strengths and limitations of this approach.

Acknowledgements

This work was supported by grant MCB 0212669 from the National Science Foundation.

References

[1] D.W. Bolen, M.M. Santoro, Unfolding free energy changes determined by the linear extrapolation method. 2. Incorporation of delta G degrees N-U values in a thermodynamic cycle, Biochemistry 27 (1988) 8069–8074.

[2] A.S. Yang, B. Honig, On the pH dependence of protein stability, J. Mol. Biol. 231 (1993) 459–474.

[3] B.S. McCrary, J. Bedell, S.P. Edmondson, J.W. Shriver, Linkage of protonation and anion binding to the folding of Sac7d, J. Mol. Biol. 276 (1998) 203–224.
[4] B. Garcia-Moreno, Probing structural and physical basis of protein energetics linked to protons and salt, Methods Enzymol. 259 (1995) 512–538.
[5] M. Straume, E. Freire, Two-dimensional differential scanning calorimetry: simultaneous resolution of intrinsic protein structural energetics and ligand binding interactions by global linkage analysis, Anal. Biochem. 203 (1992) 259–268.
[6] D.R. Ripoll, Y.N. Vorobjev, A. Liwo, J.A. Vila, H.A. Scheraga, Coupling between folding and ionization equilibria: effects of pH on the conformational preferences of polypeptides, J. Mol. Biol. 264 (1996) 770–783.
[7] A.L. Creagh, J. Koska, P.E. Johnson, P. Tomme, M.D. Joshi, L.P. McIntosh, D.G. Kilburn, C.A. Haynes, Stability and oligosaccharide binding of the N1 cellulose-binding domain of Cellulomonas fimi endoglucanase CenC, Biochemistry 37 (1998) 3529–3537.
[8] C.H. Henkels, J.C. Kurz, C.A. Fierke, T.G. Oas, Linked folding and anion binding of the Bacillus subtilis ribonuclease P protein, Biochemistry 40 (2001) 2777–2789.
[9] G.K. Ackers, Deciphering the molecular code of hemoglobin allostery, Adv. Protein Chem. 51 (1998) 185–253.
[10] J.A. Schellman, Macromolecular binding, Biopolymers 14 (1975) 999–1018.
[11] J.A. Schellman, Selective binding and solvent denaturation, Biopolymers 26 (1987) 549–559.
[12] J.F. Maune, C.B. Klee, K. Beckingham, Ca^{2+} binding and conformational change in two series of point mutations to the individual Ca(2+)-binding sites of calmodulin, J. Biol. Chem. 267 (1992) 5286–5295.
[13] S. Pedigo, M.A. Shea, Quantitative endoproteinase GluC footprinting of cooperative Ca^{2+} binding to calmodulin: proteolytic susceptibility of E31 and E87 indicates interdomain interactions, Biochemistry 34 (1995) 1179–1196.
[14] M.A. Shea, A.S. Verhoeven, S. Pedigo, Calcium-induced interactions of calmodulin domains revealed by quantitative thrombin footprinting of Arg37 and Arg106, Biochemistry 35 (1996) 2943–2957.
[15] M. Ikura, G.M. Clore, A.M. Gronenborn, G. Zhu, C.B. Klee, A. Bax, Solution structure of a calmodulin–target peptide complex by multidimensional NMR, Science 256 (1992) 632–638.
[16] B.R. Sorensen, M.A. Shea, Interactions between domains of apo calmodulin alter calcium binding and stability, Biochemistry 37 (1998) 4244–4253.
[17] L. Masino, S.R. Martin, P.M. Bayley, Ligand binding and thermodynamic stability of a multidomain protein, calmodulin, Protein Sci. 9 (2000) 1519–1529.
[18] B.R. Sorensen, L.A. Faga, R. Hultman, M.A. Shea, An interdomain linker increases the thermostability and decreases the calcium affinity of the calmodulin N-domain, Biochemistry 41 (2002) 15–20.
[19] S. Linse, A. Helmersson, S. Forsen, Calcium binding to calmodulin and its globular domains, J. Biol. Chem. 266 (1991) 8050–8054.
[20] T.N. Tsalkova, P.L. Privalov, Thermodynamic study of domain organization in troponin C and calmodulin, J. Mol. Biol. 181 (1985) 533–544.
[21] F.W. Studier, A.H. Rosenberg, J.J. Dunn, J.W. Dubendorff, Use of T7 RNA polymerase to direct expression of cloned genes, Methods Enzymol. 185 (1990) 60–89.
[22] J.A. Putkey, G.R. Slaughter, A.R. Means, Bacterial expression and characterization of proteins derived from the chicken calmodulin cDNA and a calmodulin processed gene, J. Biol. Chem. 260 (1985) 4704–4712.
[23] M.R. Nelson, W.J. Chazin, An interaction-based analysis of calcium-induced conformational changes in Ca^{2+} sensor proteins, Protein Sci. 7 (1998) 270–282.
[24] C.B. Klee, Conformational transition accompanying the binding of Ca^{2+} to the protein activator of 3′,5′-cyclic adenosine monophosphate phosphodiesterase, Biochemistry 16 (1977) 1017–1024.
[25] R.E. Klevit, Spectroscopic analyses of calmodulin and its interactions, Methods Enzymol. 102 (1983) 82–104.
[26] C.N. Pace, Determination and analysis of urea and guanidine hydrochloride denaturation curves, Methods Enzymol. 131 (1986) 266–280.
[27] R.F. Greene Jr., C.N. Pace, Urea and guanidine hydrochloride denaturation of ribonuclease, lysozyme, alpha-chymotrypsin, and beta-lactoglobulin, J. Biol. Chem. 249 (1974) 5388–5393.
[28] M.M. Santoro, D.W. Bolen, Unfolding free energy changes determined by the linear extrapolation method. 1. Unfolding of phenylmethanesulfonyl alpha-chymotrypsin using different denaturants, Biochemistry 27 (1988) 8063–8068.
[29] A. Prasad, N.A. Housley, S. Pedigo, Thermodynamic stability of domain 2 of epithelial cadherin, Biochemistry 43 (2004) 8055–8066.
[30] R. Tsien, T. Pozzan, Measurement of cytosolic free Ca^{2+} with quin2, Methods Enzymol. 172 (1989) 230–262.
[31] Y.S. Babu, C.E. Bugg, W.J. Cook, Structure of calmodulin refined at 2.2 A resolution, J. Mol. Biol. 204 (1988) 191–204.
[32] M. Ikura, S. Spera, G. Barbato, L.E. Kay, M. Krinks, A. Bax, Secondary structure and side-chain ^{1}H and ^{13}C resonance assignments of calmodulin in solution by heteronuclear multidimensional NMR spectroscopy, Biochemistry 30 (1991) 9216–9228.
[33] J.F. Maune, K. Beckingham, S.R. Martin, P.M. Bayley, Circular dichroism studies on calcium binding to two series of Ca^{2+} binding site mutants of *Drosophila melanogaster* calmodulin, Biochemistry 31 (1992) 7779–7786.
[34] S. Fefeu, R.R. Biekofsky, J.E. McCormick, S.R. Martin, P.M. Bayley, J. Feeney, Calcium-induced refolding of the calmodulin V136G mutant studied by NMR spectroscopy: evidence for interaction between the two globular domains [In Process Citation], Biochemistry 39 (2000) 15920–15931.
[35] J.P. Browne, M. Strom, S.R. Martin, P.M. Bayley, The role of beta-sheet interactions in domain stability, folding, and target recognition reactions of calmodulin, Biochemistry 36 (1997) 9550–9561.
[36] N.J. Greenfield, G.D. Fasman, Computed circular dischroism spectra for protein conformation, Biochemistry 8 (1969) 4108–4116.
[37] X. Wu, R.E. Reid, Structure/calcium affinity relationships of site III of calmodulin: testing the acid pair hypothesis using calmodulin mutants, Biochemistry 36 (1997) 8649–8656.
[38] N.C. Strynadka, M.N. James, Crystal structures of the helix-loop-helix calcium-binding proteins, Annu. Rev. Biochem. 58 (1989) 951–998.
[39] M.T. Henzl, R.C. Hapak, J.J. Likos, Interconversion of the ligand arrays in the CD and EF sites of oncomodulin. Influence on Ca^{2+}-binding affinity, Biochemistry 37 (1998) 9101–9111.
[40] J.K. Myers, C.N. Pace, J.M. Scholtz, Denaturant m values and heat capacity changes: relation to changes in accessible surface areas of protein unfolding [published erratum appears in Protein Sci 1996 May; 5(5):981], Protein Sci. 4 (1995) 2138–2148.
[41] S. Miller, J. Janin, A.M. Lesk, C. Chothia, Interior and surface of monomeric proteins, J. Mol. Biol. 196 (1987) 641–656.
[42] C.L. Wang, R.R. Aquaron, P.C. Leavis, J. Gergely, Metal-binding properties of calmodulin, Eur. J. Biochem. 124 (1982) 7–12.
[43] M.C. Kilhoffer, M. Kubina, F. Travers, J. Haiech, Use of engineered proteins with internal tryptophan reporter groups and pertubation techniques to probe the mechanism of ligand–protein interactions: investigation of the mechanism of calcium binding to calmodulin, Biochemistry 31 (1992) 8098–8106.
[44] A. Babu, H. Su, Y. Ryu, J. Gulati, Determination of residue specificity in the EF-hand of troponin C for Ca^{2+} coordination, by genetic engineering [published erratum appears in J Biol Chem 1992 Nov 15;287(32):23434], J. Biol. Chem. 267 (1992) 15469–15474.
[45] I. Matsuura, E. Kimura, K. Tai, M. Yazawa, Mutagenesis of the fourth calcium-binding domain of yeast calmodulin, J. Biol. Chem. 268 (1993) 13267–13273.
[46] M.A. Starovasnik, D.R. Su, K. Beckingham, R.E. Klevit, A series of point mutations reveal interactions between the calcium-binding sites of calmodulin, Protein Sci. 1 (1992) 245–253.

[47] M.A. Starovasnik, T.N. Davis, R.E. Klevit, Similarities and differences between yeast and vertebrate calmodulin: an examination of the calcium-binding and structural properties of calmodulin from the yeast *Saccharomyces cerevisiae*, Biochemistry 32 (1993) 3261–3270.
[48] L.A. Faga, B.R. Sorensen, W.S. VanScyoc, M.A. Shea, Basic interdomain boundary residues in calmodulin decrease calcium affinity of sites I and II by stabilizing helix–helix interactions, Proteins 50 (2003) 381–391.
[49] R.B. Martin, in: H. Sigel (Ed.), Bioinorganic Chemistry of Calcium, Calcium and its Role in Biology, Marcel Dekker, NY, 1984, pp. 1–49.
[50] H. Einspahr, C.E. Bugg, in: H. Sigel (Ed.), Crystal Structure Studies of Calcium Complexes and Implications for Biological Systems, Calcium and its Role in Biology, Marcel Dekker, NY, 1984, pp. 51–97.
[51] R. Gilli, D. Lafitte, C. Lopez, M. Kilhoffer, A. Makarov, C. Briand, J. Haiech, Thermodynamic analysis of calcium and magnesium binding to calmodulin, Biochemistry 37 (1998) 5450–5456.
[52] D. Lafitte, J.P. Capony, G. Grassy, J. Haiech, B. Calas, Analysis of the ion binding sites of calmodulin by electrospray ionization mass spectrometry, Biochemistry 34 (1995) 13825–13832.
[53] M. Milos, M. Comte, J.J. Schaer, J.A. Cox, Evidence for four capital and six auxiliary cation-binding sites on calmodulin: divalent cation interactions monitored by direct binding and microcalorimetry, J. Inorg. Biochem. 36 (1989) 11–25.
[54] M.A. Wilson, A.T. Brunger, The 1.0 A crystal structure of Ca(2+)-bound calmodulin: an analysis of disorder and implications for functionally relevant plasticity, J. Mol. Biol. 301 (2000) 1237–1256.
[55] C. Chothia, The nature of the accessible and buried surfaces in proteins, J. Mol. Biol. 105 (1976) 1–14.
[56] J.R. Livingstone, R.S. Spolar, M.T. Record Jr., Contribution to the thermodynamics of protein folding from the reduction in water-accessible nonpolar surface area, Biochemistry 30 (1991) 4237–4244.
[57] O.V. Tsodikov, M.T. Record Jr., Y.V. Sergeev, A novel computer program for fast and exact calculation of accessible and molecular surface areas and average surface curvature, J. Comput. Chem. 23 (2002) 600–609.
[58] B.E. Finn, T. Drakenberg, S. Forsen, The structure of apo-calmodulin. A ^{1}H NMR examination of the carboxy-terminal domain, FEBS Lett. 336 (1993) 368–374.